

**TITLE PAGE**

# Solution NMR of Acetylcholine Binding Protein Reveals ACh-mediated Conformational Change of the C-loop

Fan Gao, Georges Mer, Marco Tonelli, Scott B. Hansen, Thomas P. Burghardt, Palmer Taylor, and Steven  
M. Sine

Receptor Biology Laboratory, Dept. of Physiology and Biomedical Engineering (F.G., S.M.S.), Dept. of  
Biochemistry and Molecular Biology (G.M., T.P.B.), Mayo Clinic College of Medicine, Rochester  
Minnesota 55905; Dept. of Pharmacology, Univ. of California, San Diego, La Jolla, California 92093  
(S.B.H., P.T.); National Magnetic Resonance Facility, University of Wisconsin, Madison, Wisconsin  
53706 (M. T.)

MOL 27185

**RUNNING TITLE PAGE**

TITLE RUNNING HEAD: NMR reveals conformational change of AChBP C-loop

CORRESPONDING AUTHOR: Steven M. Sine, Receptor Biology Laboratory, Dept. of Physiology and Biomedical Engineering, Mayo Clinic College of Medicine, Rochester Minnesota 55905. Phone: 507 284 9404; Fax: 507 284 9420; E-Mail: [sine@mayo.edu](mailto:sine@mayo.edu).

THE NUMBER OF TEXT PAGES: 20

THE NUMBER OF TABLES: 1

THE NUMBER OF FIGURES: 4

THE NUMBER OF REFERENCES: 28

THE NUMBER OF WORDS IN ABSTRACT: 227

THE NUMBER OF WORDS IN INTRODUCTION: 660

THE NUMBER OF WORDS IN RESULTS: 751

THE NUMBER OF WORDS IN DISCUSSION: 902

ABBREVIATIONS: AChBP, acetylcholine binding protein; ACh, acetylcholine; TROSY, transverse relaxation optimized spectroscopy; HEK, human embryonic kidney.

MOL 27185

## ABSTRACT

Previous x-ray crystallography, molecular dynamics simulation, fluorescence spectroscopy and deuterium-hydrogen exchange of acetylcholine binding protein (AChBP) suggest that following binding of the agonist, the C-loop at the periphery of the binding site draws inward to cap the site and envelop the agonist. Here we use high-resolution solution NMR to monitor changes in the chemical environment of the C-loop without and with ACh bound. Substitution of  $^{15}\text{N}$ -cysteine for the native cysteines 123, 136, 187, and 188 provided intrinsic monitors of the chemical environments of the Cys- and C-loops, respectively. Two-dimensional TROSY  $^{15}\text{N}$ - $^1\text{H}$  HSQC spectroscopy of apo AChBP reveals seven well-resolved cross-peaks for the group of cysteines. The spectrum of AChBP with Ser substituted for Cys 187 and 188 shows only two main cross-peaks, corresponding to Cys 123 and 136 from the Cys-loop, enabling resonance assignments. Following binding of ACh, the five cross-peaks associated with cysteines from the C-loop condense into two predominant cross-peaks not observed in the spectrum from the apo protein, indicating a restricted range of conformations and change in chemical environment of the C-loop. The results show that isotopic cysteine can be incorporated into specified positions of AChBP expressed from a eukaryotic source, that the C-loop assumes multiple conformations without ACh, but that its conformation becomes restricted with ACh bound. The collective findings suggest a structural mechanism for agonist recognition in AChBP and related Cys-loop receptors.

## INTRODUCTION

Recognition of a neurotransmitter by its receptor is the first step in generating the post-synaptic response. Conformational changes associated with neurotransmitter recognition are expected in theory, but for rapidly activated synaptic receptors, they remain to be characterized experimentally. The crystal structure of AChBP (Brejc et al., 2001; Celie et al., 2004; Hansen et al., 2005) has emerged as a prototype for understanding structures of ligand binding domains from the Cys-loop superfamily of neurotransmitter receptors (Sine, 2002; Sixma and Smit, 2003). AChBP shows sequence homology to all members of the Cys-loop receptor superfamily, and its three-dimensional structure closely fits that of the extracellular ligand binding region of the acetylcholine receptor from the *Torpedo* electroplaque (Unwin et al., 2002; Unwin, 2005). Further, the pharmacology of AChBP is typical of a cholinergic receptor, binding small agonists and antagonists (Smit et al., 2001; Hansen et al., 2002),  $\alpha$ -conotoxins (Hansen et al., 2005, Celie et al., 2005), and  $\alpha$ -neurotoxins (Bourne et al., 2005). AChBP may therefore serve as a good model for investigating conformational changes associated with agonist recognition in Cys-loop receptors.

Detecting conformational changes presents special challenges for a protein the size of AChBP, which contains five identical subunits of 28 kD each. Fluorescence spectroscopy provides high sensitivity and single residue precision, and has been used to monitor ligand-mediated changes in intrinsic Trp fluorescence of AChBP (Hansen et al., 2002; Gao et al., 2005) and in fluorophore-conjugated AChBP (Hibbs et al., 2004). However fluorescence studies require the fluorophore to be structurally compatible at the site of incorporation, and for extrinsic fluorophores, the native structure is altered. Solution NMR, on the other hand, maintains the native structure, and use of multiple dimensions allows resolution of resonances associated with any residue. Further, the rapid signal decay inherent to large proteins can be overcome by the transverse relaxation optimized spectroscopy (TROSY) technique, which selects the most slowly decaying resonances (Pervushin, 2000; Fiaux et al., 2002; Riek et al., 2002).

Ligand-dependent conformational changes in AChBP have been inferred from crystal structures with bound agonists or peptide toxins. With either nicotine or carbamylcholine bound to AChBP, the C-loop at the

MOL 27185

periphery of the binding site is situated closer to the aromatic-rich center compared to the structure without agonist (Celie et al., 2004). However the agonist-free structure contains HEPES in the binding site, which may serve as a ligand and promote a partial change in conformation, thus obscuring the true apo protein structure (Hansen et al., 2005). With either  $\alpha$ -conotoxins (Hansen et al., 2005; Celie et al., 2005) or  $\alpha$ -neurotoxin (Bourne et al., 2005) bound, the peripheral C-loop is displaced away from the binding site center, suggesting conformational mobility of the C-loop.

Starting with the HEPES-bound structure of AChBP, molecular dynamics simulation also reveals a large outward displacement of the C-loop, which is prevented when ACh is bound (Gao et al., 2005). This uncapped conformation of the C-loop is similar to that in the 4 Å resolution structure of the Torpedo receptor (Unwin, 2005), to that from molecular dynamics simulation of a homology model of the homomeric  $\alpha 7$  receptor (Law et al., 2005), and to that in the crystal structure of the apo form of an AChBP ortholog from *Aplysia* (Hansen et al., 2005). Fluorescence of AChBP with acrylodan conjugated at Gln 178 at the base of the C-loop reveals a ligand-mediated change in environment from hydrophobic to hydrophilic, suggesting conformational change in this region (Hibbs et al., 2004). Finally when ACh is bound to AChBP, a pair of essential Trp residues deep in the binding pocket shows reduced accessibility to an extrinsic quencher of Trp fluorescence (Gao et al., 2005), and five of the amide hydrogens in the C-loop show reduced exchange with solvent (Shi et al., 2006). Thus the collective studies provide indirect evidence that the C-loop changes from uncapped to capped conformations upon binding the agonist. Here we use two-dimensional TROSY  $^{15}\text{N}$ - $^1\text{H}$  HSQC spectroscopy to directly monitor chemical environments of the C-loop with and without ACh bound.

## MATERIALS AND METHODS

*Expression, isotopic labeling, and purification of AChBP from 293 HEK cells-* The previously described stable cell line expressing AChBP from *Lymnaea stagnalis* was used for large-scale protein expression (Hansen et al., 2002). It was generated from 293 HEK cells transfected with the expression vector CMV-9 (Sigma-Aldrich, St. Louis, MO) containing the AChBP coding sequence and an N-terminal 3x FLAG tag sequence, followed by selection with geneticin (Invitrogen, Carlsbad, CA). A cDNA encoding AChBP with the double mutation C187S & C188S was generated using the QuickChange kit (Stratagene, La Jolla, CA), confirmed by dideoxy sequencing, and was stably incorporated into 293 HEK cells in the same manner.

To incorporate  $^{15}\text{N}$ -labeled L-cysteine at selective sites in AChBP, cells from the stable cell line were maintained at 37 °C in DMEM (Invitrogen, Carlsbad, CA) supplemented with fetal bovine serum (FBS, 10 % v/v, Hyclone, Logan, UT) until 70 % confluence was achieved. The medium was then replaced by DMEM lacking L-cysteine and L-methionine (Invitrogen, Carlsbad, CA) and supplemented with  $^{15}\text{N}$ -labeled L-cysteine (50 mg/l, Cambridge Isotopes, Andover, MA), unlabeled L-methionine (30 mg/l, Sigma-Aldrich, St. Louis, MO), and dialyzed FBS (10 % v/v, Hyclone, Logan, UT). After incubation at 31 °C for 6 days, the culture medium was collected, centrifuged, and passed through a column containing agarose-coupled anti-FLAG M2 antibody (Sigma-Aldrich, St. Louis, MO). The protein was eluted in Tris-buffered saline (50 mM Tris HCl, 150 mM NaCl, pH 7.4) containing the 3x FLAG peptide and further purified by FPLC size exclusion chromatography (Superdex 200, Pharmacia, London, UK).

*NMR spectroscopy of AChBP-* AChBP was concentrated to 10 mg/ml in a volume of about 300  $\mu\text{l}$  containing 50 mM Tris HCl, 150 mM NaCl, 5 % v/v  $\text{D}_2\text{O}$ , pH 7.4. All NMR experiments were run at the National Magnetic Resonance Facility, University of Wisconsin, Madison, on a Varian Inova spectrometer operating at 800 MHz and equipped with a cryogenic probe. The sample was placed in a Shigemi sample tube, and two-dimensional spectra were recorded at 31°C using a TROSY- $^{15}\text{N}$ - $^1\text{H}$  heteronuclear single quantum correlation (HSQC) pulse sequence (Kay et al., 1992; Weigelt, 1998) from the Varian BioPack library of sequences, and optimized at NMRFAM for use with the cryogenic probe. Usually, 256 to 512 scans were averaged for each

MOL 27185

of the 72 complex points collected in the indirect  $^{15}\text{N}$  dimension, resulting in a total acquisition time of 12 to 24 hours. The proton carrier frequency was set at the water resonance, while the nitrogen carrier was set at 127 ppm and the  $^{15}\text{N}$  spectral window narrowed to 22 ppm to optimize the resolution with the least number of points. The spectra were processed and analyzed using nmrPipe/nmrDraw software (Delaglio et al., 1995).

*Tryptophan fluorescence measurements-* Wild-type or mutant AChBP in 50 mM Tris HCl, 150 mM NaCl, pH 7.4 was stored on ice and placed in a 3 x 3 mm cuvette in a PTI fluorescence spectrometer (PTI, Birmingham, NJ) and maintained at 4 °C as described (12). Steady-state fluorescence was measured using an excitation wavelength of  $298 \pm 2$  nm and an emission wavelength of 342 nm. The normalized fluorescence intensity change (F) was plotted as a function of ACh concentration.

## RESULTS

Molecular dynamics simulation of AChBP revealed a progressive opening of the binding pocket in which the C-loop that caps the pocket in the HEPES-, nicotine-, and carbamylcholine-bound structures (Celie et al., 2004) moves outward to uncap the pocket (Gao et al., 2005). The tip of the C-loop harbors a pair of disulfide-linked cysteines, 187 and 188, which are expected to encounter substantially different environments between uncapped and capped conformations (Fig. 1). Only two other cysteines are present in each subunit, at positions 123 and 136, but these localize to the Cys-loop remote from the binding pocket. We therefore reasoned that selective labeling of AChBP with  $^{15}\text{N}$ -L-cysteine should produce NMR spectra with a small number of cross-peaks, and that a subset of these should change chemical shift following binding of the agonist.

A two-dimensional  $^{15}\text{N}$ - $^1\text{H}$  TROSY HSQC spectrum from apo AChBP labeled with  $^{15}\text{N}$ -L-Cysteine was recorded for 12 hours at 31 °C using an 800 MHz spectrometer (Fig. 2). The protein was stable under the temperature and buffer conditions employed, as revealed by FPLC size exclusion chromatography, which showed a single mono-disperse peak that was superimposable before and after recording multiple spectra (Fig. 3). The apo form of AChBP exhibits seven strong cross peaks in the spectral region shown in Fig. 2. A minimum of four cross peaks is expected, one for each of the four  $^{15}\text{N}$ -labeled cysteines, but additional cross peaks could arise from cis-trans isomerization of the disulfide bonds (Otting et al., 1993), multiple conformations, or non-equivalent positioning of the five identical subunits. The relatively small number of cross peaks suggests that all three mechanisms are not likely in play simultaneously.

To distinguish the cross peaks corresponding to cysteines in the C- and Cys-loops, we generated isotopically-labeled AChBP in which Ser was substituted for cysteines 187 and 188 in the C-loop. FPLC size exclusion chromatography revealed identical elution profiles for the mutant and wild type proteins (Fig. 3), and the elution profile of the mutant was unchanged following acquisition of the spectra, as observed for wild type AChBP. Moreover, measurements of intrinsic Trp fluorescence show that the mutant protein retains the ability to bind ACh, although with lower affinity. Unexpectedly, fluorescence of the mutant protein increases upon binding ACh, whereas fluorescence of the wild type protein decreases (Fig. 3).



The 2D TROSY  $^{15}\text{N}$ - $^1\text{H}$  HSQC spectrum of the mutant AChBP shows two main cross peaks. One of these falls within the spectral region displayed in Fig. 4 (left), while the other is off scale and corresponds to the solitary peak centered at 135.3 ppm ( $^{15}\text{N}$ ) and 7.7 ppm ( $^1\text{H}$ ) of the wild-type AChBP spectrum in Fig. 2. Computation of  $^{15}\text{N}$  chemical shifts based on the AChBP crystal structure predicts an 8 to 9 ppm chemical shift of the  $^{15}\text{N}$  resonance of Cys-136 from the Cys-loop relative to resonances of cysteines in the C-loop (Table 1), in qualitative agreement with the spectrum in Fig. 2. Thus the two cross peaks in the mutant spectrum correspond to cysteines 123 and 136 of the Cys-loop. Moreover, these two cross peaks coincide with two cross peaks observed in the wild type spectrum (Fig. 4), enabling assignment of resonances corresponding to cysteines in the C-loop of wild type AChBP. The presence of only two cross-peaks in the spectrum from the mutant AChBP shows that the five cross peaks assigned to the C-loop in wild type AChBP do not result from metabolic scrambling of the cysteine.

Following addition of ACh to wild type AChBP, cross peaks in the 2D TROSY  $^{15}\text{N}$ - $^1\text{H}$  HSQC spectrum change markedly (Fig. 4). The five cross peaks assigned to the C-loop in the apo-AChBP spectrum condense into two sharp cross peaks with strong intensity and a third cross peak with weak intensity; chemical shifts of these resonances are distinct from any observed in the apo-AChBP spectrum (compare the two upper panels in Fig. 4). Two additional cross peaks are observed, but these coincide precisely with cross peaks observed in the mutant spectrum following addition of ACh (compare upper and lower panels in Fig. 4, right), and thus correspond to cysteines in the Cys-loop.

The spectral changes with ACh bound provide direct evidence that the apex of the C-loop of AChBP changes chemical environment in response to binding the agonist. In the apo-AChBP spectrum, the multiple cross-peaks show that the C-loop experiences a variety of distinct environments, perhaps due to several interchangeable conformations. However in the ACh-bound spectrum, the reduced number of cross-peaks indicates the apex of the C-loop experiences more limited conformational mobility.

## DISCUSSION

We used solution NMR to assess changes in chemical environment of the C-loop at the periphery of the ligand binding pocket of AChBP in response to binding ACh. The experiments were made possible by large-scale expression of AChBP from a stable eukaryotic cell line, selective incorporation of  $^{15}\text{N}$  cysteine into the C- and Cys-loops, and high-resolution 2D heteronuclear TROSY spectroscopy. The results complement those from x-ray crystallography of liganded AChBP (Celie et al., 2004; Hansen et al., 2005; Celie et al., 2005; Bourne et al., 2005), molecular dynamics simulation of AChBP (Gao et al., 2005), fluorescence of acrylodan-conjugated AChBP (Hibbs et al., 2004), ACh-mediated changes in accessibility of binding site Trps to an extrinsic fluorescence quencher (Gao et al., 2005), and changes in deuterium-hydrogen exchange in response to ligand binding (Shi et al., 2006). The collective findings clarify how the C-loop of AChBP contributes to agonist recognition, and suggest how this may translate into a picture of agonist recognition in Cys-loop receptors.

High-resolution NMR provides several advantages over x-ray crystallography and fluorescence spectroscopy for detecting protein conformational changes. The protein is maintained in soluble form where it can freely explore conformational space. In contrast, the conformation in a crystal may differ from those predominant in solution, and the different conformational states may be difficult to arrest in crystal form. Fluorescence relies on either intrinsic Trp residues, incorporation of unnatural fluorescent amino acids, or covalent conjugation of thiol- or amino-reactive fluorophores. NMR on the other hand, allows selection of the amino acid for isotopic labeling, and maintains the native structure. In AChBP studied here, cysteine is present at only four positions per homomeric subunit of the native structure, and two positions localize to a region thought to undergo a substantial change in conformation.

The spectrum from apo AChBP shows five distinct cross peaks associated with cysteines 187 and 188 of the C-loop, whereas only two cross peaks are expected. The presence of multiple cross peaks indicates a range of distinct conformations, presumably similar in nature to the uncapped conformation observed by x-ray crystallography and molecular dynamics simulation (Fig. 1). Cis-trans isomerization about the disulfide

MOL 27185

bond (Otting et al., 1993) or different conformations of the equivalent subunits could also give rise to multiple cross peaks in apo AChBP. Prolonged molecular dynamics simulations show that bound ACh reduces asymmetry and restricts mobility of the main chain of AChBP (Gao et al., 2005) and the alpha7 ligand binding domain (Henchman et al., 2003), which may explain the restricted range of conformations indicated by the presence of only two main cross peaks in the ACh-bound spectrum.

A recent study examined deuterium-hydrogen exchange of AChBP, without and with bound agonists, followed by enzymatic digestion and mass spectrometric identification of a fragment containing the C-loop (Shi et al., 2006). In agreement with the present results, the C-loop of apo AChBP exhibited faster and more extensive incorporation of deuterium compared to agonist-bound AChBP. The present study complements the findings from deuterium-hydrogen exchange by providing single residue precision and localizing a region of conformational mobility to the vicinal cysteines at the apex of the C-loop.

The present results directly demonstrate a change in chemical environment of the C-loop following binding of ACh in solution, but they do not indicate the direction or magnitude of the change. However, our results combine with results from x-ray crystallography, molecular dynamics simulation, and fluorescence spectroscopy to clarify our picture of how the C-loop contributes to molecular recognition of the agonist. In the agonist-free conformation, the C-loop assumes a range of interconvertible uncapped conformations, allowing access of small agonists, antagonists, and peptide toxins. When the ligand is a peptide such as  $\alpha$ -conotoxin or  $\alpha$ -neurotoxin, the C-loop remains uncapped and the toxins fill the binding pocket, preventing access of small ligands. When the ligand is a small agonist, the C-loop moves into a capped position, locking the agonist in place. This capping mechanism is reminiscent of the clamshell mechanism for agonist binding to ionotropic glutamate receptors (Gouaux 2003).

In Cys-loop receptors the capping motion of the C-loop not only aids in binding the agonist, but it may also initiate downstream conformational changes that trigger gating of the channel (Sine and Engel, 2006). The ability of an AChBP/5-HT3 chimera to open the channel in response to agonist shows that AChBP has

MOL 27185

the capacity for conformational change that opens the channel (Bouzat et al., 2004). The uncapped conformation of AChBP obtained by MD simulation shows a salt bridge between Asp 194 at the base of the C-loop and Lys 139 just after the Cys-loop (Gao and Sine, unpublished), which is also present in the crystal structure of AChBP with bound HEPES (Brejc et al., 2001; Celie et al., 2004). In the agonist-bound crystal structures, a new salt bridge forms between Tyr 185, located near the apex of the C-loop, and Lys 139, and the distance between Asp 194 and Lys 139 increases (Celie et al., 2004). In the muscle nicotinic receptor, mutations of residues homologous to these, Asp 200, Lys 145, and Tyr 190, all profoundly impair gating of the channel, suggesting that the capping motion of the C-loop relays the initial conformational change from the ACh binding site toward the channel gating machinery (Mukhtasimova et al., 2005). Thus the conformational changes of the C-loop detected here not only contribute to molecular recognition of the agonist, but also may initiate the cascade of structural rearrangements that opens the channel.

MOL 27185

## **ACKNOWLEDGMENTS**

We thank Nina Bren and Sun Huang for help with protein purification.

## REFERENCES

- Bourne Y, Talley TT, Hansen SB, Taylor P, and Marchot P (2005) Crystal structure of a Cbtx-AChBP complex reveals essential interactions between snake alpha-neurotoxins and nicotinic receptors. *EMBO J.* **24**: 1512-1522.
- Bouzat C, Gumilar F, Spitzmaul G, Wang HL, Rayes D, Hansen SB, Taylor P, and Sine SM (2004) Coupling of agonist binding to channel gating in an ACh-binding protein linked to an ion channel. *Nature* **430**: 896-900.
- Brejč K, van Dijk WJ, Klaassen RV, Schuurmans M, van Der Oost J, Smit AB, and Sixma TK (2001) Crystal structure of an ACh-binding protein reveals the ligand-binding domain of nicotinic receptors, *Nature* **411**: 269-276.
- Celie PH, van Rossum-Fikkert SE, van Dijk WJ, Brejč K, Smit AB, and Sixma TK (2004) Nicotine and carbamylcholine binding to nicotinic acetylcholine receptors as studied in AChBP crystal structures. *Neuron* **41**: 907-914.
- Celie PH, Kasheverov IE, Mordvintsev DY, Hogg RC, van Nierop P, van Elk R, van Rossum-Fikkert SE, Zhmak MN, Bertrand D, Tsetlin V, Sixma TK, and Smit AB (2005) Crystal structure of nicotinic acetylcholine receptor homolog AChBP in complex with an alpha-conotoxin PnIA variant. *Nat. Struct. Mol. Biol.* **12**: 582-588.
- Delaglio F, Grzesiek S, Vuister GW, Zhu G, Pfeifer J, and Bax A (1995) NMRPipe: a multidimensional spectral processing system based on UNIX pipes. *J. Biomol. NMR* **6**: 277-293.
- Fiaux J, Bertelsen EB, Horwich AL, and Wuthrich K (2002) NMR analysis of a 900K GroEL GroES complex *Nature* **418**: 207-211.

MOL 27185

Gao F, Bren N, Burghardt TP, Hansen SB, Henchman RH, Taylor P, McCammon JA, and Sine SM (2005) Agonist-mediated conformational change in acetylcholine binding protein revealed by simulation and intrinsic tryptophan fluorescence. *J. Biol. Chem.* **280**: 8443-8451.

Gouaux E (2003) Structure and function of AMPA receptors. *J. Physiol.* **15**: 249-253.

Hansen SB, Radic' Z, Talley TT, Molles BE, Deerinck T, Tsigelny I, and Taylor P (2002) Tryptophan fluorescence reveals conformational changes in the acetylcholine binding protein. *J. Biol. Chem.* **277**: 41299-41302.

Hansen SB, Sulzenbacher G, Huxford T, Marchot P, Taylor P, and Bourne Y (2005) Structures of Aplysia AChBP complexes with nicotinic agonists and antagonists reveal distinctive binding interfaces and conformations. *EMBO J.* **24**: 3635-3646.

Henchman RH, Wang HL, Sine SM, Taylor P, and McCammon JA (2003) Asymmetric structural motions of the homomeric alpha7 nicotinic receptor ligand binding domain revealed by molecular dynamics simulation. *Biophys. J.* **85**: 3007-3018.

Hibbs RE, Talley TT, and Taylor P (2004) Acrylodan-conjugated cysteine side chains reveal conformational state and ligand site locations of the acetylcholine-binding protein. *J. Biol. Chem.* **279**: 28483-28491.

Kay L, Keifer P, and Saarinen T (1992) Pure absorption gradient enhanced heteronuclear single quantum correlation spectroscopy with improved sensitivity. *J. Amer. Chem. Soc.* **114**: 10663-10665.

Law R, Henchman R, and McCammon JA (2005) A gating mechanism proposed from a simulation of a human alpha7 nicotinic acetylcholine receptor. *Proc. Natl. Acad. Sci.* **102**, 6813-6818.

Meiler J (2003) PROSHIFT: protein chemical shift prediction using artificial neural networks. *J. Biomol. NMR.* **26**: 25-37.

MOL 27185

Mukhtasimova N, Free C, and Sine SM (2005) Initial coupling of binding to gating mediated by conserved residues in the muscle receptor. *J. Gen. Physiol.* **126**: 23-39.

Otting G, Liepinsh E, and Wuthrich K (1993) Disulfide bond isomerization in BPTI and BPTI(G36S): an NMR study of correlated mobility in proteins. *Biochemistry* **32**: 3571-3582.

Pervushin K (2000) Impact of transverse relaxation optimized spectroscopy (TROSY) on NMR as a technique in structural biology. *Q. Rev. Biophys.* **33**: 161-197.

Riek R, Fiaux J, Bertelson EB, Horwich AL, and Wuthrich K (2002) Solution NMR techniques for large molecular and supramolecular structures. *J. Am. Chem. Soc.* **124**: 12144-12153.

Shi J, Koeppe JR, Komives EA, and Taylor P (2006) Ligand-induced conformational changes in the acetylcholine binding protein analyzed by hydrogen-deuterium exchange mass spectrometry. *J. Biol. Chem.* Published ahead of print.

Sine SM (2002) The nicotinic receptor ligand binding domain. *J. Neurobiol.* **3**: 431-446.

Sine SM and Engel AG (2006) Recent advances in Cys-loop receptor structure and function. *Nature*. **440**: 448-455.

Sixma T and Smit A (2003) Acetylcholine binding protein (AChBP): a secreted glial protein that provides a high-resolution model for the extracellular domain of pentameric ligand-gated ion channels. *Annu. Rev. Biophys. Biomol. Struct.* **32**: 311-334.

Smit AB, Syed NI, Schaap D, van Minnen J, Klumperman J, Kits KS, Lodder H, van der Schors RC, van Elk R, Sorgedraeger B, Brejc K, Sixma TK, and Geraets WP (2001) A glia-derived acetylcholine-binding protein that modulates synaptic transmission. *Nature* **411**: 261-268.

Unwin N, Miyazawa A, Li J, and Fujiyoshi Y (2002) Activation of the nicotinic acetylcholine receptor involves a switch in conformation of the alpha subunits. *J. Mol. Biol.* **319**: 1165-1176.



MOL 27185

Unwin N (2005) Refined structure of the nicotinic acetylcholine receptor at 4Å resolution. *J. Mol. Biol.* **346**: 967-989.

Weigelt J (1998) Single scan, sensitivity- and gradient-enhanced TROSY for multidimensional NMR experiments. *J. Amer. Chem. Soc.* **120**: 10778-10779.

## FOOTNOTES

This work was supported by R37 NS-31744 (SMS), AR49277 (TPB), and R37 GM18360 (PT). The National Magnetic Resonance Facility at University of Wisconsin Madison is supported by NIH grants P41RR02301 and P41GM66326.

Contacting person to receive reprint requests: Steven M. Sine, Receptor Biology Laboratory, Dept. of Physiology and Biomedical Engineering, Mayo Clinic College of Medicine, Rochester Minnesota 55905.

E-Mail: [sine@mayo.edu](mailto:sine@mayo.edu).

## LEGENDS FOR FIGURES

**Figure 1-** Superimposed *apo* (yellow) and ACh-bound (green) AChBP subunit pairs obtained by molecular dynamics simulation (Gao et al., 2005). The C-loop in the *apo* structure is highlighted in red, with Cysteines 187 and 188 shown in stick representation.

**Figure 2-** Two-dimensional TROSY HSQC- $^{15}\text{N}$ - $^1\text{H}$  spectrum of  $^{15}\text{N}$ -cysteine-labeled *apo* AChBP recorded at 800 MHz at 31°C.

**Figure 3-** FPLC of wild type and mutant AChBP and fluorescence quenching or enhancement by ACh. Panels A and B show size exclusion chromatography (0.7 ml/min) of wild type and mutant AChBP following acquisition of NMR spectra. Lower panel shows the change in steady-state fluorescence intensity of wild type and mutant AChBP following titration of ACh, normalized according to  $F=(f_{\text{ACh}}-f_0)/(f_{\text{max}}-f_0)$  where  $f_{\text{ACh}}$  is the intensity at a given concentration of ACh,  $f_0$  is the intensity before addition of ACh, and  $f_{\text{max}}$  is the asymptotic intensity as the concentration of ACh approaches a maximum. For wild type AChBP  $f_{\text{max}}/f_0$  was 0.65 (Gao et al., 2005), and that for the mutant was 1.3.

**Figure 4-** Two-dimensional TROSY HSQC- $^{15}\text{N}$ - $^1\text{H}$  spectra of  $^{15}\text{N}$ -cysteine-labeled wild type and mutant AChBP in the *apo* and ACh-bound (20 mM acetylcholine chloride) forms recorded at 800 MHz at 31°C. In all four spectra, the solitary peak at 135.3 ppm ( $^{15}\text{N}$ ) and 7.7 ppm ( $^1\text{H}$ ), visible in Fig. 2, was off scale. Asterisks indicate major cross-peaks associated with cysteines 187 and 188 of the C-loop.

**Table I-** Calculated  $^{15}\text{N}$  chemical shifts (ppm) for cysteines in AChBP

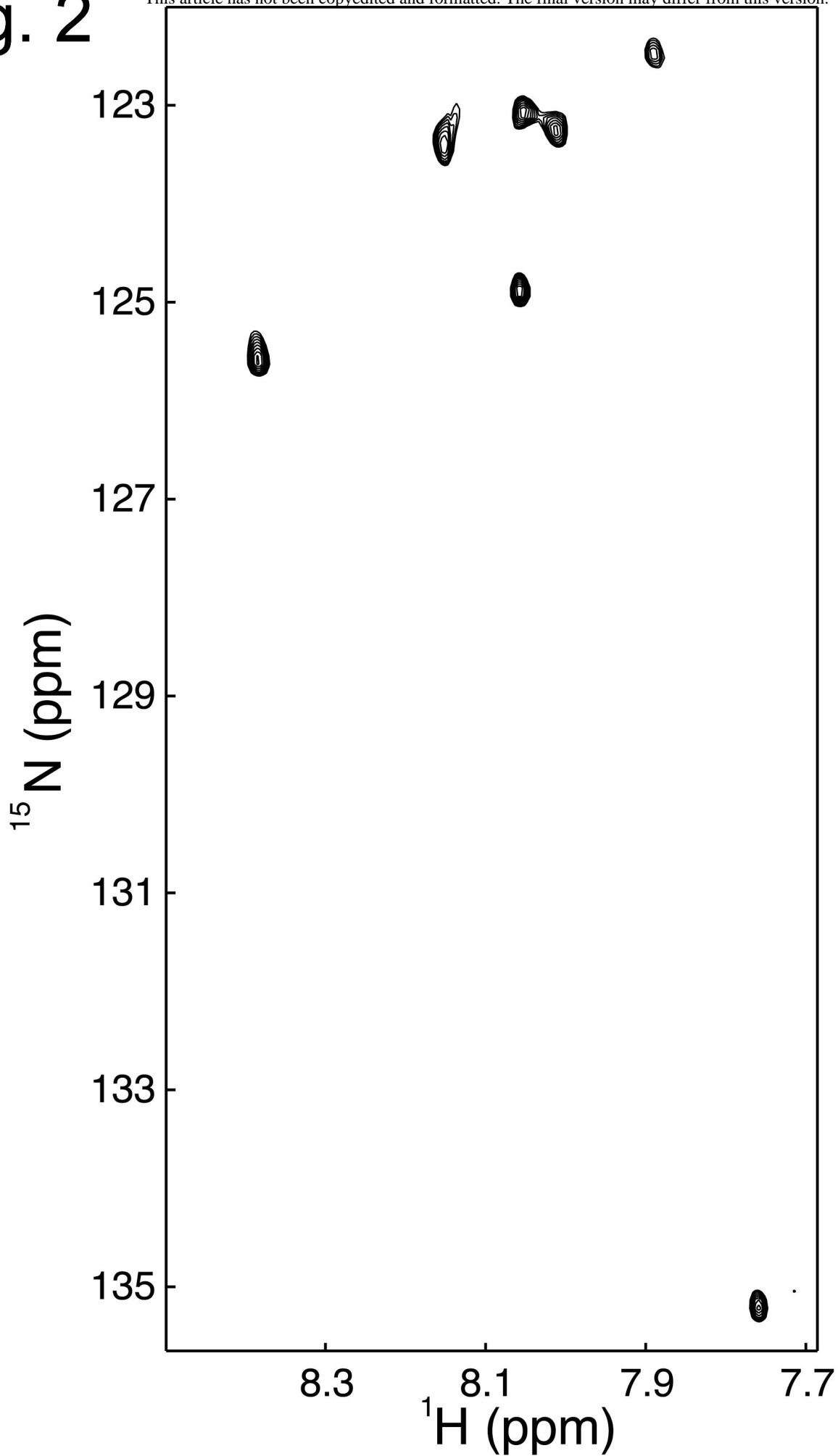
Residue number	Subunit A	Subunit B	Subunit C	Subunit D	Subunit E	Average
Cys-123	121.46	120.76	120.06	120.38	120.07	120.55
Cys-136	123.72	124.61	123.85	124.26	124.66	124.22
Cys-187	116.43	115.92	116.61	115.90	116.52	116.28
Cys-188	115.84	115.73	115.82	115.63	115.47	115.70

The program PROSHIFT (Meiler 2003) was used to compute  $^{15}\text{N}$  chemical shifts based on the AChBP crystal structure (PDB code 1I9B).

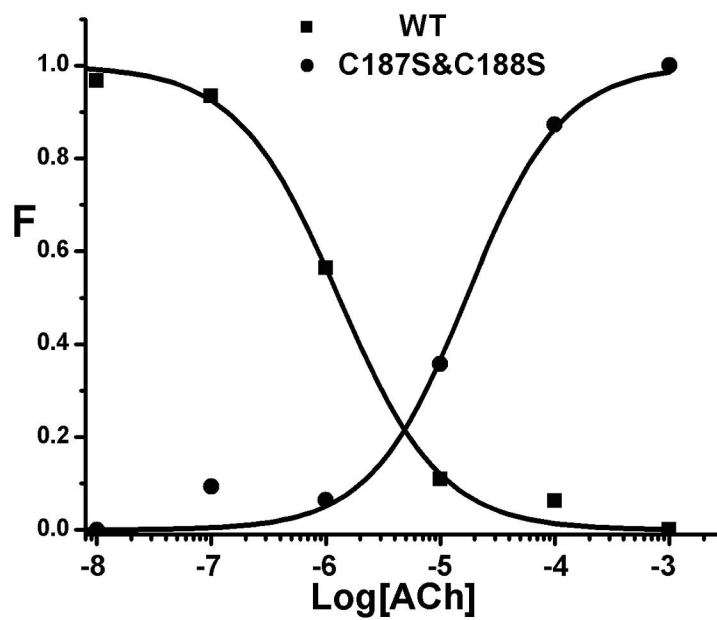
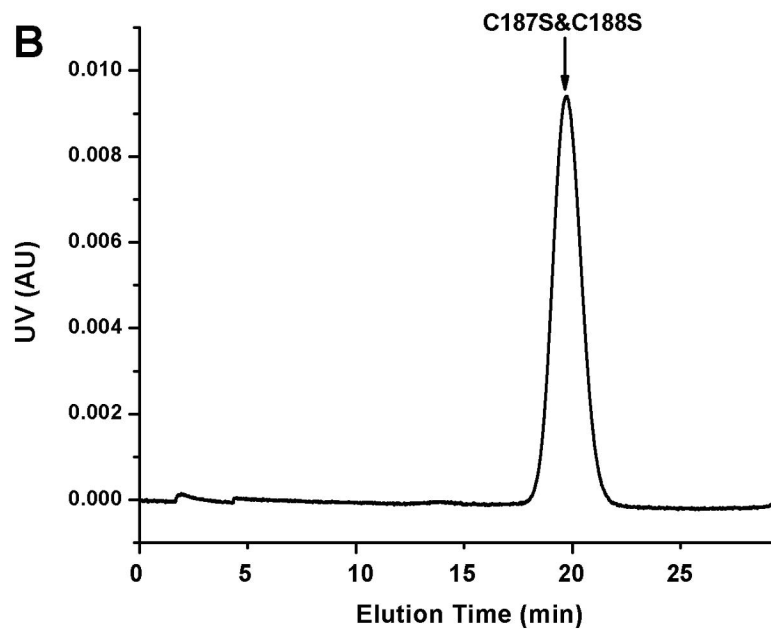
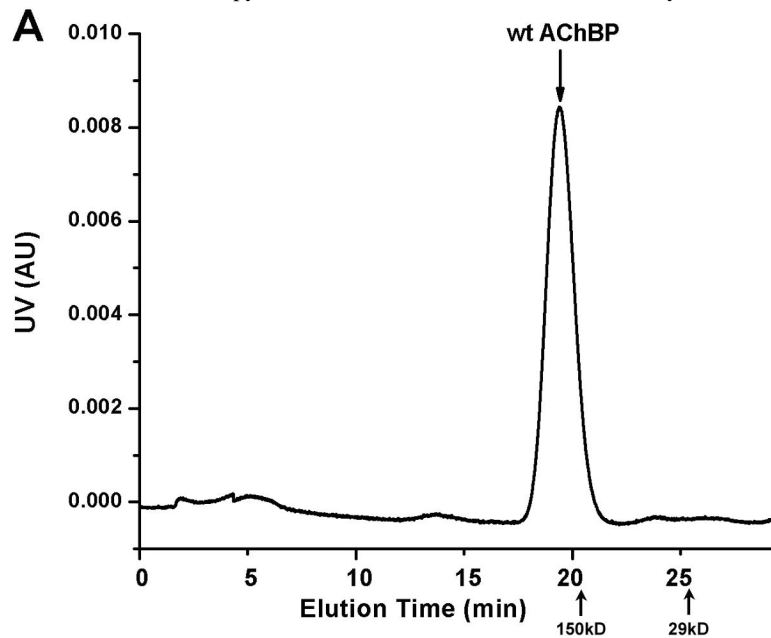
# Fig. 1



Fig. 2

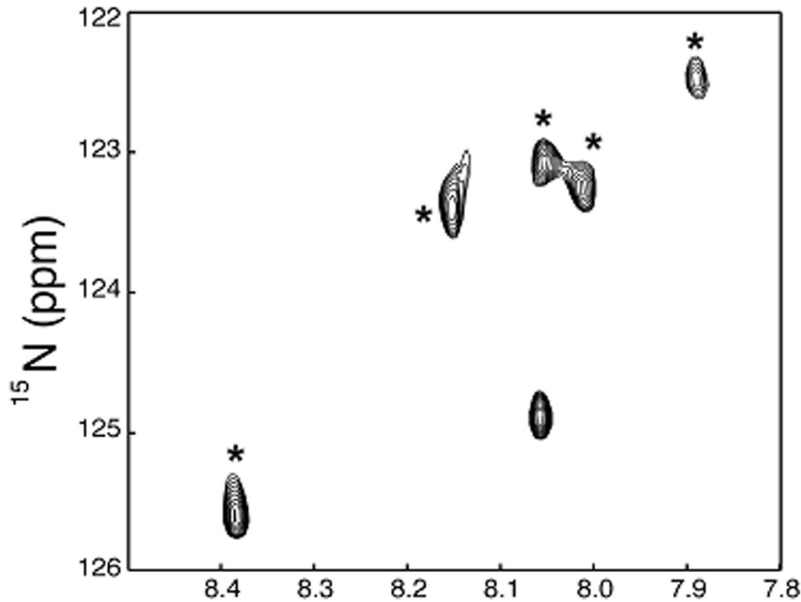


# Fig. 3

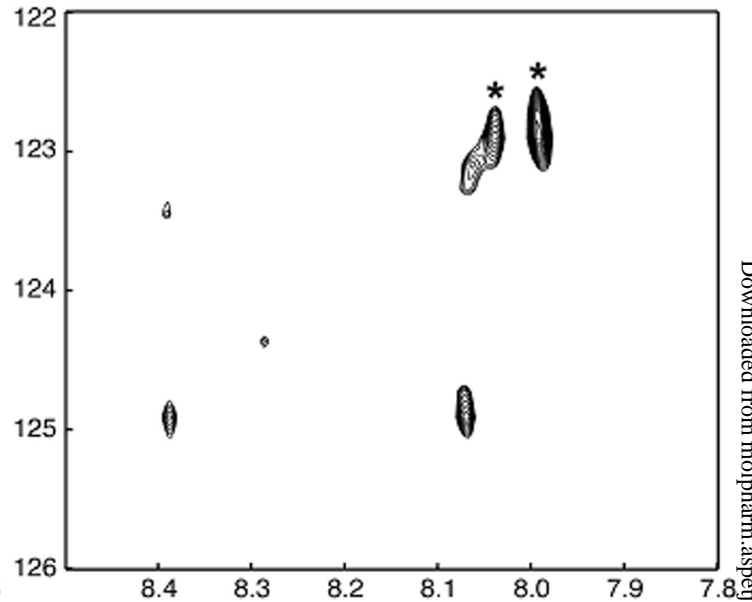


# Fig. 4

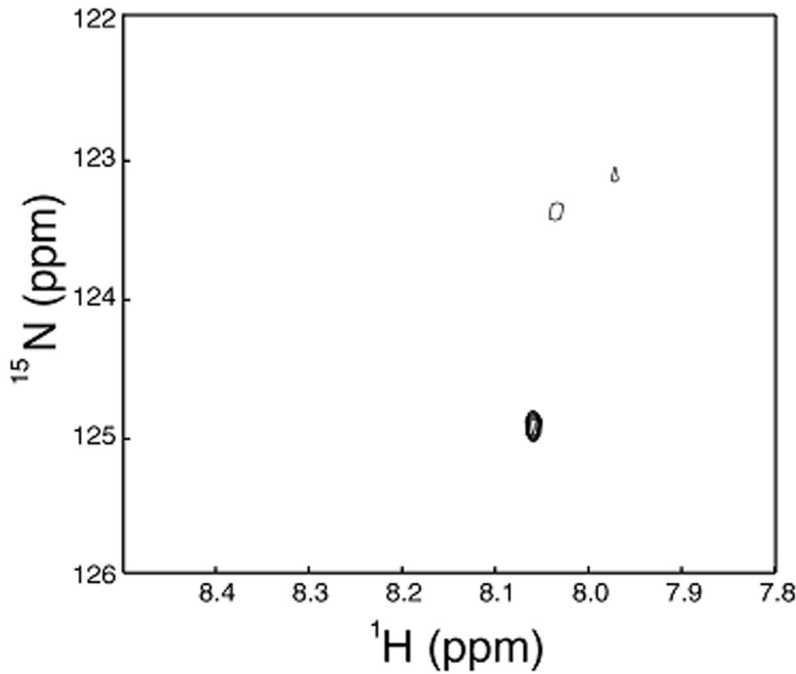
**WT apo**



**WT + ACh**



**C187S & C188S apo**



**C187S & C188S + ACh**

